Supplemental Information

Reactive uptake and photo-Fenton oxidation of glycolaldehyde in aerosol liquid water

T.B. Nguyen[1†], M.M. Coggon[2†], R.C. Flagan[2, 3], and J.H. Seinfeld[2, 3*]

1. Division of Geological and Planetary Sciences, California Institute of Technology, Pasadena, California, USA
2. Division of Engineering and Applied Science, California Institute of Technology, Pasadena, California, USA
3. Division of Chemistry and Chemical Engineering, California Institute of Technology, Pasadena, California, USA

[†]*These authors contributed equally*

**author to whom correspondence should be directed: tbn@caltech.edu*

I. Experimental details:

Experiments were performed in a 16 L glass photochemical tubular flow reactor at low Reynolds number (Re < 5) housed in a 0.6 m^3 enclosure at 25 – 28°C, under dry (relative humidity, RH < 10%) and humid (RH ~ 80%) conditions (Fig. S1) An air mass in the flow reactor behaves as a piston flow with some degree of longitudinal mixing.[1] The residence times of injected aerosol varies from 30 – 60 min, estimated from the longitudinal spread. "Steady state" concentrations were confirmed by near-constant readings displayed on analytical instrumentation downstream of the flow reactor. Varying levels of RH were achieved in the reactor by mixing dry zero air (house air filtered using a combination of molecular sieves, activated carbon, Purafil media, and Drierite) with humid injection air (RH > 90 %), which was obtained by bubbling dry zero air through heated ultra-purified water (Millipore, 18 MΩ cm) past a water trap. Temperature and RH were measured by a Vaisala HMM211 probe, calibrated prior to use in the RH range of 11 – 95 % with saturated salt solutions. Seed aerosols were mixed with the air stream in a 200 cm^3 glass mixing tube and pulled through the flow reactor at ~ 450 std. cm^3 per minute (sccm).

Dilute aqueous ammonium sulfate (AS) solutions (Acros – 0.012 M) were atomized to produce seed aerosols, either alone or with 200 μM H_2O_2 (from serial dilutions of stock 50 wt % H_2O_2 in water, Aldrich) and granular ferrous sulfate hexahydrate ($Fe(SO_4)\cdot 7H_2O$, Macron) added immediately prior to atomization such that the initial $[Fe_{(II)}]$ = 5 wt % of the inorganic mass. The composition of the atomizer solution is relevant to the measured range of soluble Fe [2, 3] and H_2O_2[4] in atmospheric aerosol, fog, and cloud water. Upon atomization at RH = 80%, the contents of the atomizer solution will be concentrated in the aerosol by a factor two orders of magnitude; however, the Fe mass ratio is not expected to change.. Gas-phase H_2O_2 was not detected by

chemical ionization mass spectrometry (CIMS) during dry and humid atomization of AS + H_2O_2 solutions (Fig. S2). Gas-phase H_2O_2, especially under dry conditions, may be lost to metal tubing or the Nafion membrane of the drier prior to particles reaching the flow reactor. We conclude that gas-phase OH formation was negligible during the course of the experiments and results are due to aqueous-phase oxidation. Four seed compositions were used for experiments: AS, AS + H_2O_2, AS + Fe, and AS + Fe + H_2O_2. In the humid experiments, the atomized wet aerosols enter the flow reactor filled with humid zero air with RH ~ 80%, such that the aerosols retain significant amounts of liquid water. In the dry experiments, the seed aerosols were dried with a Nafion membrane diffusion drier before entering the flow reactor set at RH < 10%.

Glycolaldehyde was injected into the flow reactor with a 55 sccm stream of dry zero air through heated bulb that contains ~ 0.01g of glycolaldehyde dimer (23147-58-2, Fluka, > 98% purity). For uptake experiments, particles were allowed to reach a steady state before glycolaldehyde injection. The gas-phase concentration of glycolaldehyde was monitored by CIMS. The bulb temperature was set at ~ 85°C initially to melt the white solid dimer, producing a clear viscous liquid, then sustained at ~ 76°C afterward. In particle blank experiments, a 55 sccm flow of pure N_2 is added to maintain the RH in the flow reactor.

Photochemistry within the flow reactor is initiated by eight UV-B broadband lamps with maximum emission at 310 nm (Phillips, 40W T12-UVB), mounted within the reactor enclosure. The lamp photon flux spectrum is (Fig. S3) compared with a modeled ground-level solar flux[5] at solar zenith angle = 0°. From calculated photolysis rates of H_2O_2 (J_{H2O2} =3.2 x 10^{-5} s^{-1} in the flow reactor and J_{H2O2} =9.2 x 10^{-6} s^{-1} in the atmosphere), we estimate that 1 h photolytic aging in the flow reactor equals up to 3.5 h under atmospheric clear sky tropical noon conditions with 300

DU ozone column. Aging timescales reported in this work have not been converted to atmospheric values.

If unmediated, heat from the operation of the lights increases the temperature of the flow reactor enclosure by 5 – 7°C, which causes the RH to decrease from 80 to 50 - 60%. Two additional sets of control experiments were performed to isolate the temperature effect: (1) temperature-controlled humid dark and light experiments where ΔT is kept at ±1°C with the use of an air conditioner (Fig. S2) and (2) dark experiments at elevated temperature (T = 35°C) by covering the glass flow reactor with opaque material. The increase in temperature caused by the lights did not change the concentration of AMS-measured aerosol-phase organics (from glycolaldehyde dark uptake or photooxidation), e.g., by prompting volatilization of condensed glycolaldehyde or its oxidation products from particles. . We conclude that composition changes in this work are well-correlated with the production of OH and change in aerosol liquid water – not the temperature. Therefore, aerosol composition data were corrected according only to the ratio of aerosol liquid water content (R_{LWC}) at the operational temperature (27 – 32°C) in relation to the LWC at room temperature, e.g., org wt.% = $(mass)_{org}$ / $[(mass)_{total} \cdot R_{LWC}]$. The resulting values correspond to the wt% of organics in LWC of deliquesced AS particles at RH 80% and T = 27°C. LWC was calculated based on hygroscopicity measurements of ultrafine AS.[6] The flow reactor was thoroughly flushed between each series of experiments. The exit flow was analyzed for its gas-phase composition and dried with a Nafion diffusion drier before particle composition characterization.

Gas-phase measurements

Gas-phase glycolaldehyde was measured with negative ion chemical ionization mass spectrometry (CIMS) using CF_3O^- as the reagent ion.[7-9] The ions were detected using a modified Varian triple-quadrupole spectrometer with unit mass resolution and 2 – 5 min time resolution. The flow of analyte gas to the CIMS was restricted to ~ 160 sccm via a glass frit, and was carried to the ion-molecule reaction region by a flow of ~ 1600 sccm N_2 dilution gas to minimize loss of organics in the 1.5 m (0.632 cm OD) perfluoroalkoxy Teflon line. The operational pressure was approximately 26.6 Torr.

Glycolaldehyde can be monitored by its cluster ion $C_2H_4O_2 \cdot CF_3O^-$ (*m/z* 145), which in the absence of acetic acid, is entirely representative of the glycolaldehyde concentration. A water-dependent calibration of glycolaldehyde was performed in the operational RH range (25 – 2300 ppmv water in the CIMS ion molecule flow region). Aliquots were injected from fresh solutions of glycolaldehyde dimer in reagent-grade methanol into an inflatable Teflon bag filled with zero air of varying RH. The sensitivity of glycolaldehyde was not observed to be significantly water-dependent in the operational RH range, in good agreement with previous reports.[10]

Particle-phase measurements

Particle size and number concentrations were measured with a custom-built column and radial mobility analyzer (CARMA) coupled to a butanol condensation particle counter (CPC). The CARMA-CPC was calibrated with polystyrene latex (PSL) spheres. The particles entering the flow reactor have a static polydisperse distribution, with a peak in the particle diameter distribution at D_p ~ 40 nm (Fig. S4). The mass concentration of AS particles typically ranges

from 5 – 25 μg m^{-3} for all experiments. Due to slightly variable inorganic seed concentrations, all composition measurements are normalized to the total particle mass.

Particle composition was measured with an aerosol mass spectrometer using a high-resolution time-of-flight mass analyzer (ToF-AMS, Aerodyne Research Inc.) in V mode (R ~ 3000 – 4000 at *m/z* 200). Data were analyzed in IGOR Pro (WaveMetrics, Inc., Lake Oswego, Oregon, USA) using the SQUIRREL v 1.51H and PIKA v 1.10H analysis toolkits. Gas interferences and elemental ratios were calculated using the fragmentation table developed by Allan et al.[11] and Aiken et al.[12] Prior to experiments, the ToF-AMS ionization efficiency was calibrated using size-selected 350 nm ammonium nitrate particles. CHO^+ (m/z 29) and CH_4O^+ (m/z 32), two peaks with strong interferences from common air species were omitted in our analysis due to possible errors in the correction process (Fig.S5 and associated discussion). Consequently, the O/C ratios of organics may be biased low. The elemental ratios reported in this work are used primarily as a metric for comparison between different oxidation mechanisms.

II. Possible competition from direct photolysis:

The effective glycolaldehyde OH rate coefficient can be calculated in the aqueous phase using a structure-reactivity relationship [13] (k_{eff} = 7.8 x 10 $^{-4}$ s^{-1}) or assuming a gas-phase reaction rate coefficient,[14] (k_{eff} = 5.6 x 10 $^{-3}$ s^{-1}). Glycolaldehyde may also be photolyzed directly through the Norrish I mechanism as a competing reaction in the presence of irradiation,[15] and we calculate $J_{glycolald.}$ = 1.1 x 10^{-4} s^{-1} in the flow reactor using the gas-phase absorption cross section[16] and a quantum yield of unity. Due to the uncertainty in the aqueous OH rate coefficient and photolysis rate, the relative importance of direct photolysis of glycolaldehyde may range from unimportant (< 2%) to moderately competitive (~ 14%). In this work, we do not consider the direct photolysis in data interpretation.

Table S1: Results of uptake and oxidation from experiments with dry seeds (seed water < 5%), analogous to results shown in Table 1. Figure 3 shows that organics do not uptake onto the dry seeds, which causes significant error in determining the organic weight % and elemental rations, due to low organic signal-to-noise.

Experiment	Net org. (wt %)	<H/C>	<O/C>	<N/C>
AS + org	-4.5 (± 5)	1.7	0.2	<0.01
AS + H_2O_2 + org	-6.3 (± 5)	1.7	0.2	<0.01
AS + H_2O_2 + org + hν	-1.8 (± 5)	1.6	0.4	<0.01
AS + Fe(II) + org	1.3 (± 5)	1.6	0.3	<0.01
AS + Fe(II) + H_2O_2 + org	2.4 (± 5)	1.6	0.4	<0.01
AS + Fe(II)+ H_2O_2 + org + hν	4.6 (± 5)	1.5	0.6	<0.01

Figure S1: Diagram of photochemical flow reactor set up for typical experiment.

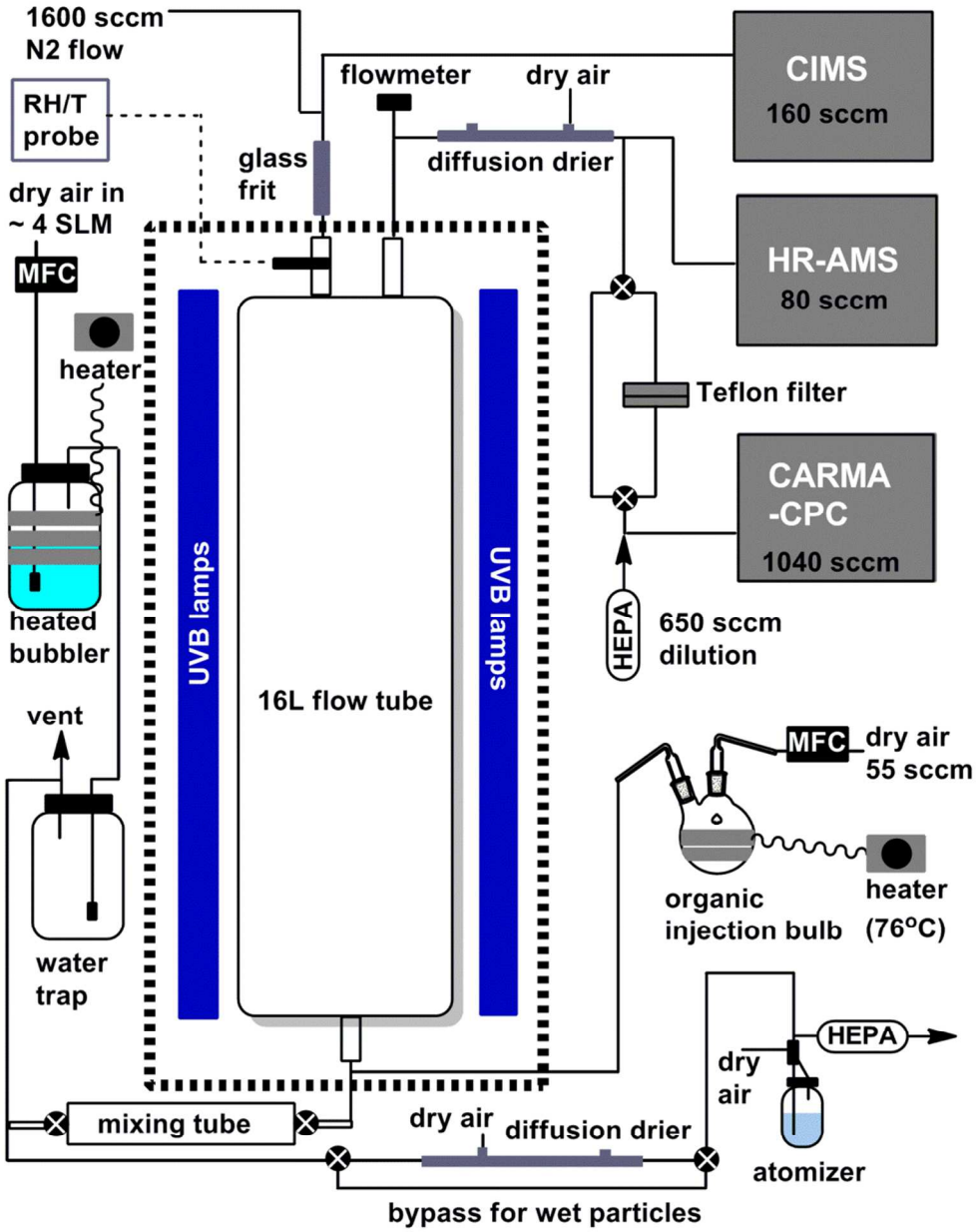

Figure S2: CIMS spectra and time profile of tracers for H_2O_2 in the gas phase during atomization blanks performed with high flow rates (~ 3.5 SLM), assuring that gas-phase H_2O_2 in the flow reactor will be accurately sampled by CIMS. The water ion serves as a tracer for changing RH in the flow reactor between runs. The amount of AS in the flow reactor was 15 – 20 μg m^{-3} for these tests. The H_2O_2 time-dependent tracer signal (m/z 119) is negligible during dry or humid atomization of AS + H_2O_2 solution (0.012M AS with 200 μM initial H_2O_2) using the protocol we described in the text. We believe this is because we atomize through a Nafion membrane tube (when we use it for drying we turn on a cross-flow of dry air) in order to reduce the number of particles entering the flow reactor. The Nafion membrane and the metal tubing used to introduce particles into the flow reactor may have caused peroxide loss. Notes: for peaks with very high intensities, e.g., the reagent ion CF_3O^-, we measure the ^{13}C analog only and no background correction was performed.

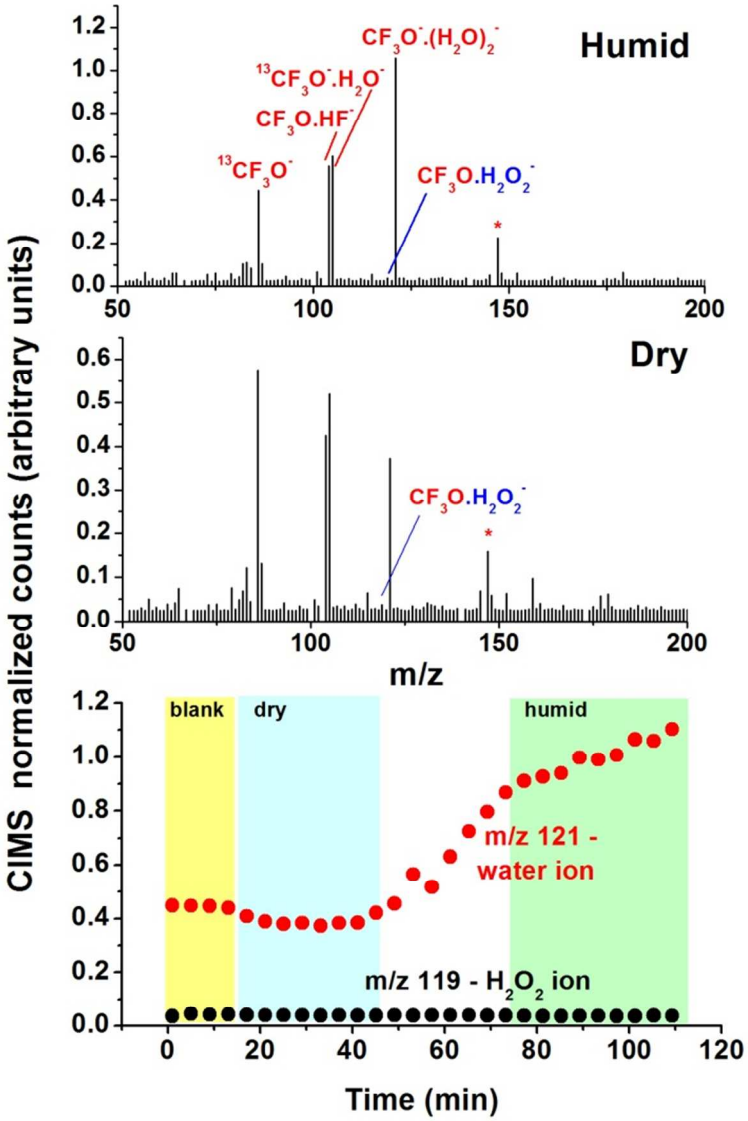

Figure S3: Spectrum of UV lamps measured from the middle of the flow tube, averaged in 6 directions (red trace) compared to a modeled solar spectrum assuming clear sky conditions.

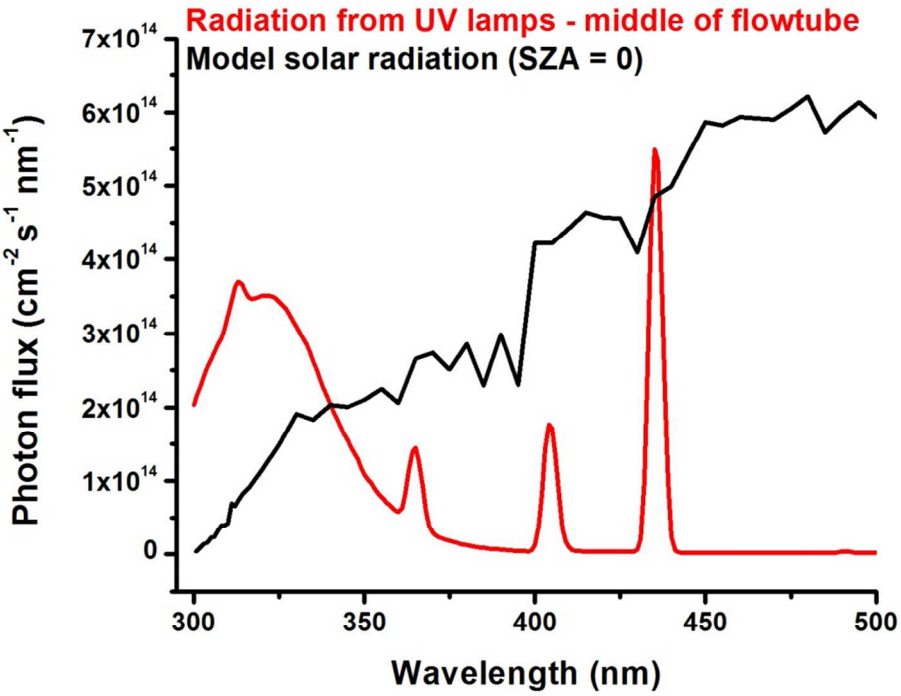

Figure S4: Temperature rises due to operation of lights – unmediated or controlled by commercial air conditioner.

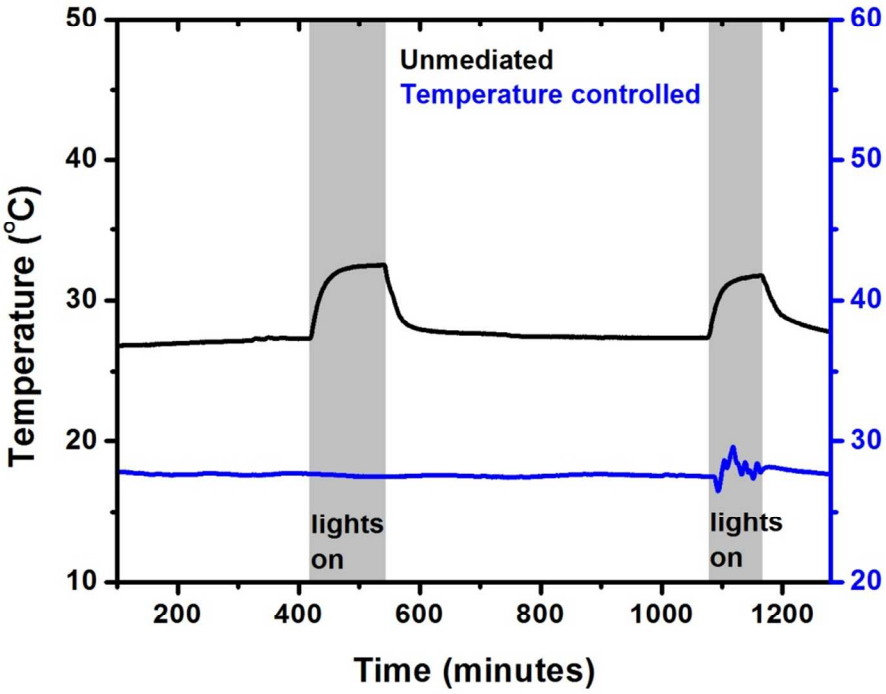

Figure S5: Particle size distribution for a typical experiment.

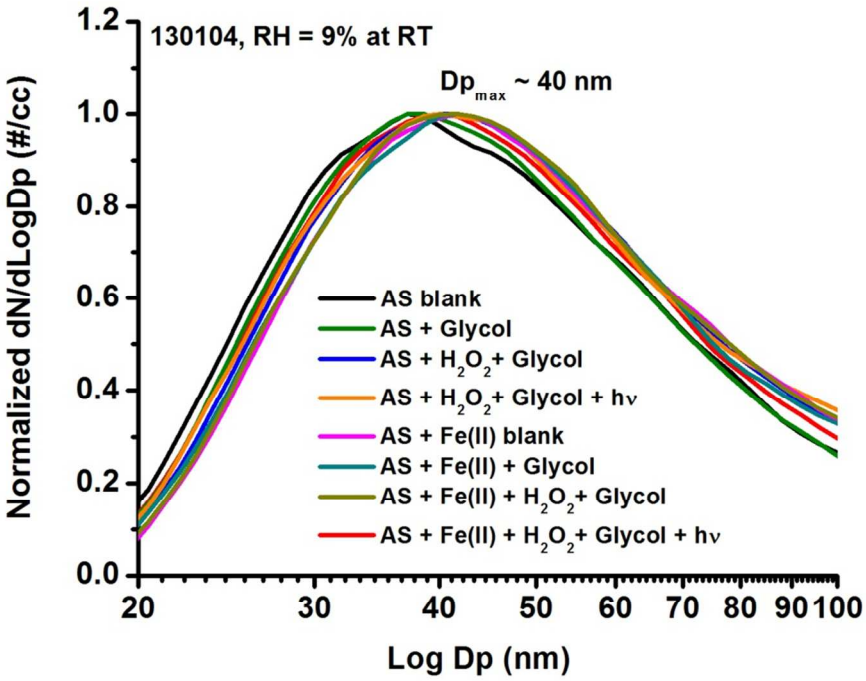

Figure S6: Detection of CHO^+ (m/z 29) and CH_4O^+ (m/z 32) suffer interferences from common air species in AMS. It is possible to correct for these interferences: for example, CHO^+ has interference by ^{15}NN, which may be estimated based on measurements of N_2 (m/z 28) and constrained by the isotopic abundance of ^{15}N. However, in our experiments, the organic loadings were low (on the order of 1 μg m^{-3} organics) and because of this, the ratio of m/z29 to m/z 28 is 0.007023, which is very close to the isotopic abundance of ^{15}NN (0.0074). Therefore, we chose not to fit CHO+ because there will be high errors associated with this correction in our work. As the focus of the work is on relative enhancements of oxidation (O/C), we believe the message can be conveyed without the inclusion of CHO^+ and CH_4O^+, even though they are significant peaks in the glycolaldehyde EI mass spectrum (Fig. 1a).

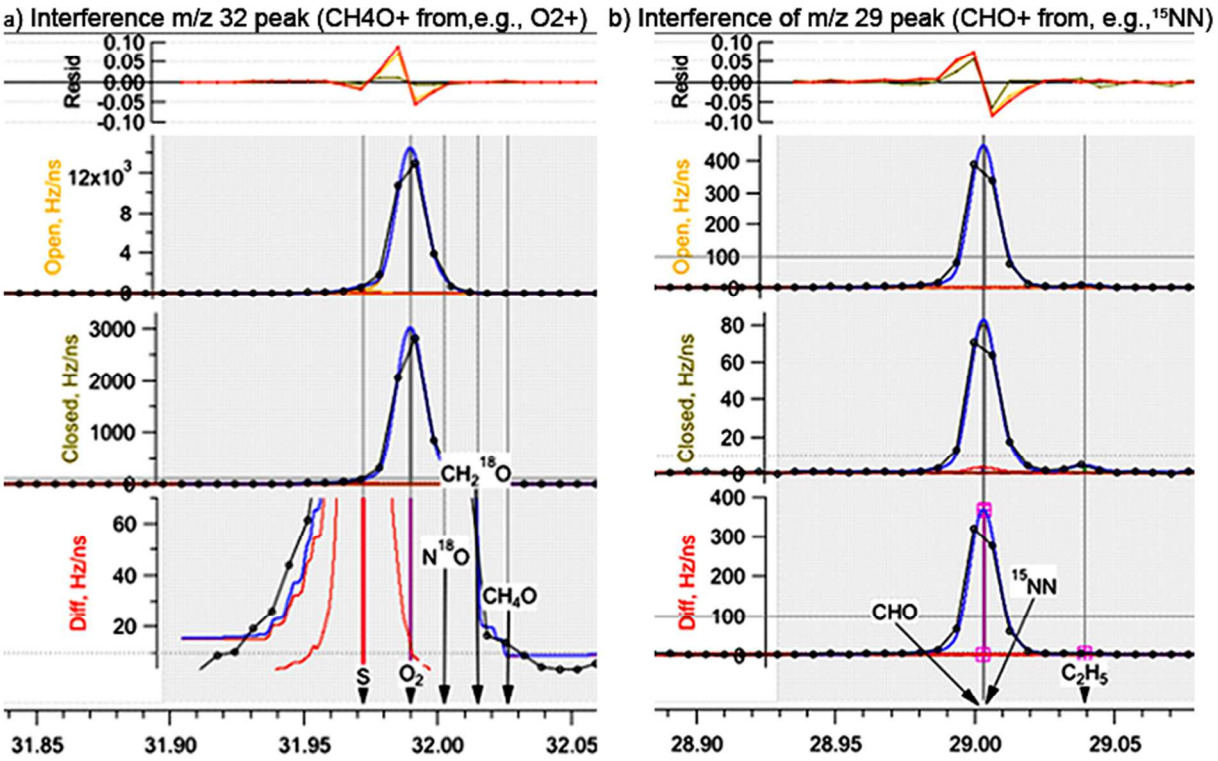

Figure S7: Representative correlation plot between CH_4N^+ (amine/imine tracer) and CH_3O^+ (glycolaldehyde tracer) in the dark uptake of glycolaldehyde onto wet ammonium sulfate seed aerosols. Similar correlation is observed in AS+Fe seeds, although the slopes are different (see relative intensities in Fig. 1 of the main text). These tracers have not been calibrated in AMS for mass, thus an absolute yield may not be extracted from the correlation plots.

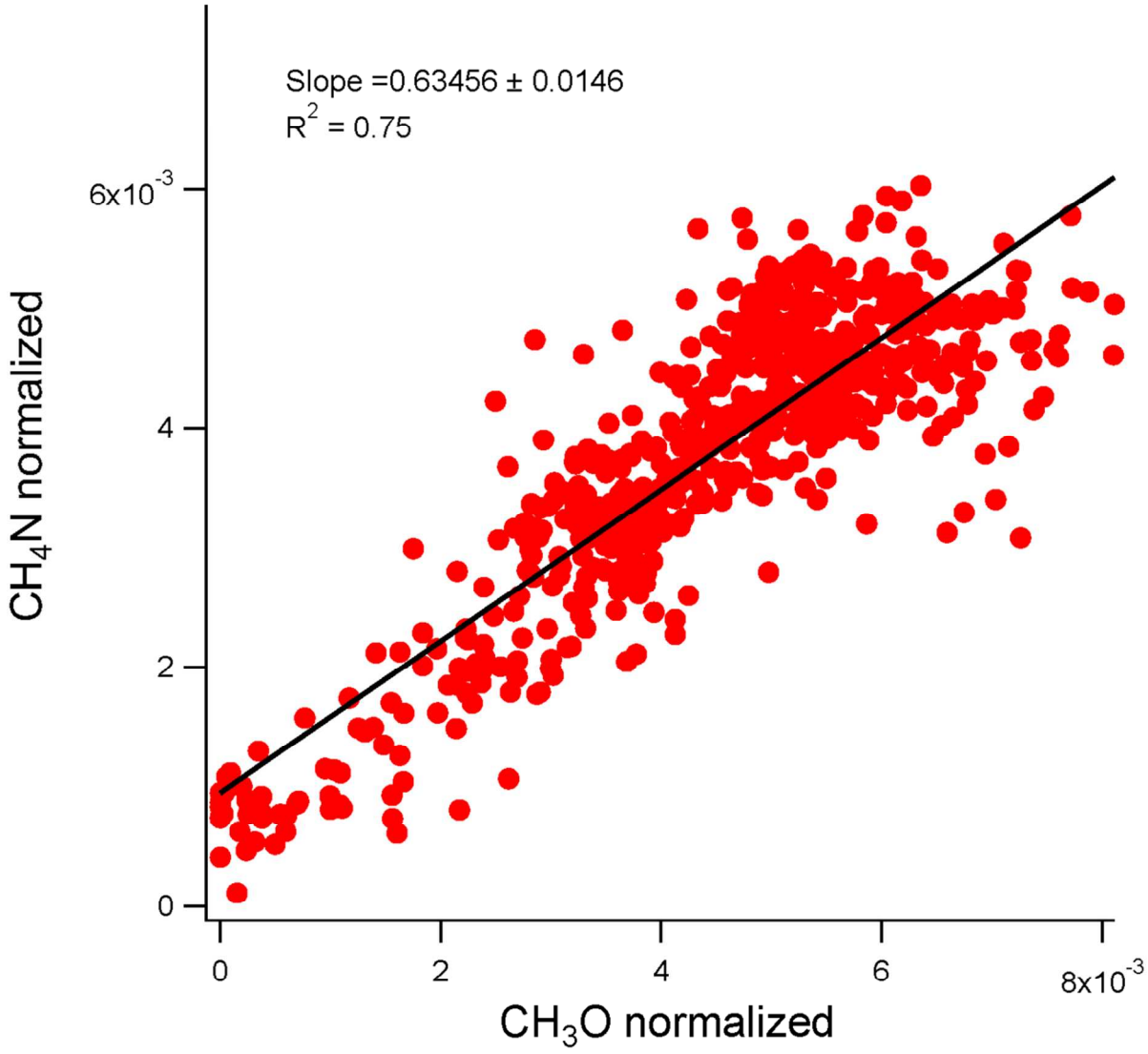

Figure S8: Comparison of "triangle" plots for experiments performed with (a) dry seed aerosol (seed water content < 5%) and (b) hydrated seed aerosols (seed water content 165 – 200%). Figure B is also shown in the main text as Figure 4. The low "organic" signal-to-noise in the dry experiments produces the significant amount of scatter seen in (a).

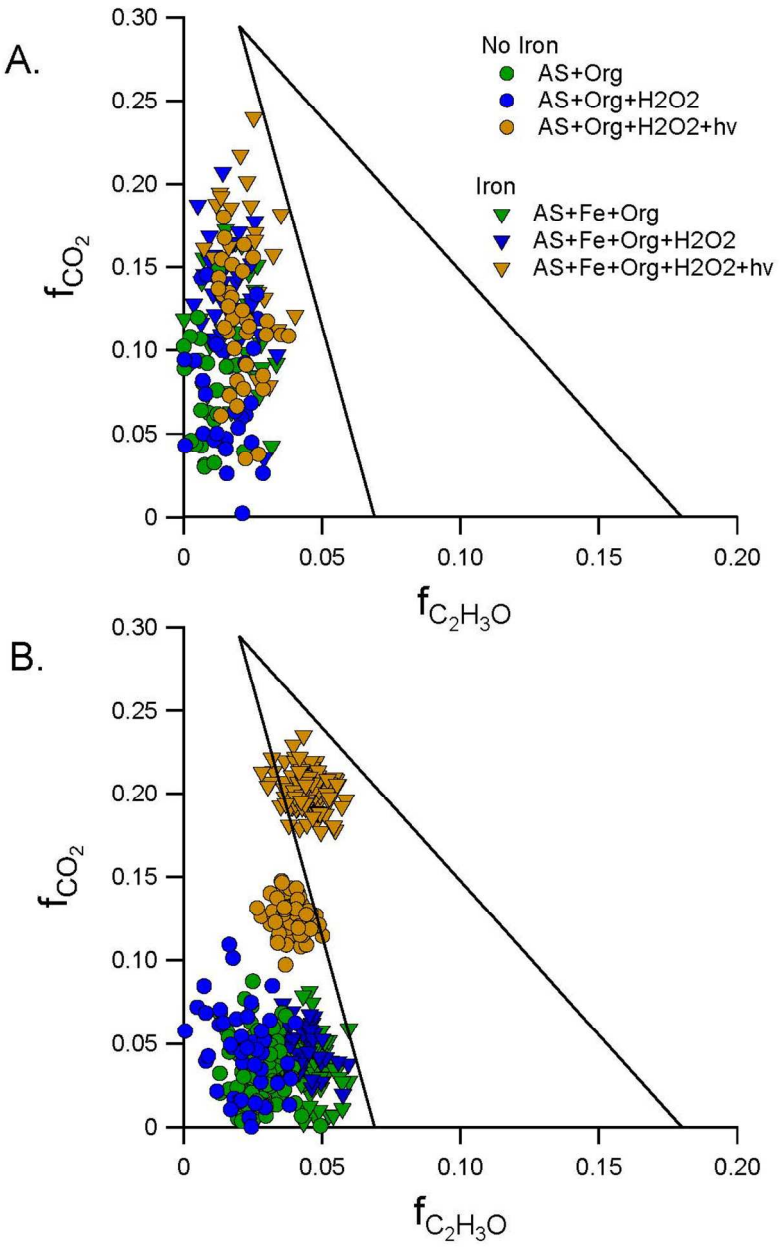

References

1. Danckwerts, P., Continuous flow systems: distribution of residence times. *Chemical Engineering Science* **1953,** *2*, (1), 1-13.
2. Hoffmann, P.; Dedik, A.; Ensling, J.; Weinbruch, S.; Weber, S.; Sinner, T.; Gütlich, P.; Ortner, H., Speciation of iron in atmospheric aerosol samples. *J. Aerosol. Sci.* **1996,** *27*, (2), 325-337.
3. Dedik, A.; Hoffmann, P.; Ensling, J., Chemical characterization of iron in atmospheric aerosols. *Atmos. Environ.* **1992,** *26*, (14), 2545-2548.
4. Gunz, D. W.; Hoffmann, M. R., Atmospheric chemistry of peroxides: a review. *Atmos. Environ.* **1990,** *24*, (7), 1601-1633.
5. Tie, X.; Madronich, S.; Walters, S.; Zhang, R.; Rasch, P.; Collins, W., Effect of clouds on photolysis and oxidants in the troposphere. *J. Geophys. Res.* **2003,** *108*, (D20), 4642; doi:10.1029/2003JD003659
6. Hameri, K.; Vakeva, M.; Hansson, H.-C.; Laaksonen, A., Hygroscopic growth of ultrafine ammonium sulphate aerosol measured using an ultrafine tandem differential mobility analyzer. *J. Geophys. Res.* **2000,** *105*, (D17), 22231-22242.
7. Crounse, J. D.; McKinney, K. A.; Kwan, A. J.; Wennberg, P. O., Measurement of Gas-Phase Hydroperoxides by Chemical Ionization Mass Spectrometry. *Anal. Chem.* **2006,** *78*, (19), 6726-6732.
8. St. Clair, J. M.; McCabe, D. C.; Crounse, J. D.; Steiner, U.; Wennberg, P. O., Chemical ionization tandem mass spectrometer for the in situ measurement of methyl hydrogen peroxide. *Rev. Sci. Instrum.* **2010,** *81*, (9), 094102-6.
9. Paulot, F.; Crounse, J. D.; Kjaergaard, H. G.; Kroll, J. H.; Seinfeld, J. H.; Wennberg, P. O., Isoprene photooxidation: new insights into the production of acids and organic nitrates. *Atmos. Chem. Phys.* **2009,** *9*, 1479-1501.
10. Spencer, K. M.; Beaver, M. R.; Clair, J. M. S.; Crounse, J. D.; Paulot, F.; Wennberg, P. O., Quantification of hydroxyacetone and glycolaldehyde using chemical ionization mass spectrometry. *Atmos. Chem. Phys. Discuss.* **2011,** *11*, (8), 23619-23653.
11. Allan, J. D.; Delia, A. E.; Coe, H.; Bower, K. N.; Alfarra, M. R.; Jimenez, J. L.; Middlebrook, A. M.; Drewnick, F.; Onasch, T. B.; Canagaratna, M. R., A generalised method for the extraction of chemically resolved mass spectra from Aerodyne aerosol mass spectrometer data. *J. Aerosol. Sci.* **2004,** *35*, (7), 909-922.
12. Aiken, A. C.; Decarlo, P. F.; Kroll, J. H.; Worsnop, D. R.; Huffman, J. A.; Docherty, K. S.; Ulbrich, I. M.; Mohr, C.; Kimmel, J. R.; Sueper, D.; Sun, Y.; Zhang, Q.; Trimborn, A.; Northway, M.; Ziemann, P. J.; Canagaratna, M. R.; Onasch, T. B.; Alfarra, M. R.; Prevot, A. S. H.; Dommen, J.; Duplissy, J.; Metzger, A.; Baltensperger, U.; Jimenez, J. L., O/C and OM/OC ratios of primary, secondary, and ambient organic aerosols with high-resolution time-of-flight aerosol mass spectrometry. *Environ. Sci. Technol.* **2008,** *42*, (12), 4478-4485.
13. Monod, A.; Doussin, J. F., Structure-activity relationship for the estimation of OH-oxidation rate constants of aliphatic organic compounds in the aqueous phase: alkanes, alcohols, organic acids and bases. *Atmos. Environ.* **2008,** *42*, (33), 7611-7622.
14. Magneron, I.; Mellouki, A.; Le Bras, G.; Moortgat, G. K.; Horowitz, A.; Wirtz, K., Photolysis and OH-Initiated oxidation of glycolaldehyde under atmospheric conditions. *J. Phys. Chem. A* **2005,** *109*, (20), 4552-4561.
15. Norrish, R. G. W.; Bamford, C. H., Photodecomposition of aldehydes and ketones. *Nature* **1937,** *140*, 195-6.
16. Bacher, C.; Tyndall, G. S.; Orlando, J. J., The Atmospheric Chemistry of Glycolaldehyde. *J. Atmos. Chem.* **2001,** *39*, (2), 171-189.